JACS
JOURNAL OF THE AMERICAN CHEMICAL SOCIETY

Communication

Artificial Molecular Pump Operating in Response to Electricity and Light

Qing-Hui Guo, Yunyan Qiu, Xinyi Kuang, Jiaqi Liang, Yuanning Feng, Long Zhang, Yang Jiao, Dengke Shen, R. Dean Astumian, and J. Fraser Stoddart

J. Am. Chem. Soc., **Just Accepted Manuscript** • DOI: 10.1021/jacs.0c06663 • Publication Date (Web): 31 Jul 2020

JOURNAL OF THE AMERICAN CHEMICAL SOCIETY

Artificial Molecular Pump Operating in Response to Electricity and Light

Qing-Hui Guo,[†,§] Yunyan Qiu,[†,§] Xinyi Kuang,[†] Jiaqi Liang,[†] Yuanning Feng,[†] Long Zhang,[†] Yang Jiao,[†] Dengke Shen,[†] R. Dean Astumian,*[,‡] and J. Fraser Stoddart*[,†,¥,#]

[†]*Department of Chemistry, Northwestern University, 2145 Sheridan Road, Evanston, Illinois 60208, United States*

[‡]*Department of Physics, University of Maine, 5709 Bennet Hall, Orono, Maine 04469, United States*

[¥]*Institute for Molecular Design and Synthesis, Tianjin University, 92 Weijin Road, Nankai District, Tianjin 300072, China*

[#]*School of Chemistry, University of New South Wales, Sydney, NSW 2052, Australia*

*E-mail: astumian@maine.edu stoddart@northwestern.edu

[§]These authors contributed equally to this work

MAIN TEXT

***Correspondence Address**

Professor J Fraser Stoddart

Department of Chemistry

Northwestern University

2145 Sheridan Road

Evanston, IL 60208 (USA)

Email: stoddart@northwestern.edu

ABSTRACT: The ability to control the relative motions of component parts in molecules is essential for the development of molecular nanotechnology. The advent of mechanically interlocked molecules (MIMs) has enhanced significantly the opportunities for chemists to harness such motions in artificial molecular machines (AMMs). Recently, we have developed artificial molecular pumps (AMPs) capable of producing highly energetic oligo- and polyrotaxanes with high precision. Here, we report the design, synthesis, and operation of an AMP incorporating a photocleavable stopper that allows for the use of orthogonal stimuli. Our approach employs a ratchet mechanism to pump a ring onto a collecting chain, forming an intermediate [2]rotaxane. At a subsequent time, application of light triggers the release of the ring back into the bulk solution with temporal control. This process is monitored by the quenching of the fluorescence of a naphthalene-based fluorophore. This design may find application in the fabrication of molecular transporting systems with on-demand functions.

■ MAIN TEXT

Biomolecular machines,[1] such as transmembrane ion-pumps,[2] use energy to control directional transport of ions across membranes. Operation of these machines is necessary for the maintenance of many other biological functions. Sophisticated and highly efficient biomolecular machines[1b] have long been a source of motivation to physical scientists to emulate their functions by designing and constructing artificial molecular counterparts.[3] The burgeoning of research on wholly synthetic molecular machines[4]—built from the bottom-up on the nanometer scale—has been one of the results of this effort to emulate biology. The past three decades have witnessed the synthesis of unnatural compounds[5] that are capable of executing controlled relative motions within their molecules. Mechanically interlocked molecules[6] (MIMs), particularly switchable rotaxanes[7] and catenanes[8], have become a focal point for the design and synthesis of artificial molecular machines[9] (AMMs). The mechanical bond[10] in MIMs permit their component parts to translocate relatively long distances in a controlled manner. The flexibility with which different units can be arranged in the MIMs allows for the systematic design of machine-like functions.

The fundamental principles governing[9b,11] these controlled relative motions in MIMs rely on switchable noncovalent bonding interactions[12] and can be induced by a range of external stimuli, e.g., chemicals,[8d,8e,13] electricity,[14] and light.[15]. Electricity[14]- and light[15]-driven AMMs[16] represent synthetic targets with the appealing advantages of ease of operation and elimination of waste products. In addition, the use[15] of light to trigger structural changes, associated with the AMMs, offers[16] spatial and temporal control. Here, we report a rotaxane-based linear molecular pump that unidirectionally transports a ring, powered[16] by an orthogonal combination of electrical and optical stimuli. Previously, we have utilized[14b,17] chemical and electrochemical redox stimuli to power the operation of artificial molecular pumps (AMPs),

creating a locally high concentration of cyclobis(paraquat-*p*-phenylene) (**CBPQT**$^{4+}$) rings on a collecting chain.

Herein, we describe the design, synthesis (Scheme 1) and operation (Figure 1) of a dumbbell-shaped AMP with a pumping cassette[18] on one end and terminated by a photocleavable stopper at the other end. When stimulated sequentially by electricity and light, the **CBPQT**$^{4+}$ ring undergoes unidirectional transport onto, along the collecting chain and off from the other end of the dumbbell, forming an intermediate [2]rotaxane **R**$^{7+}$ along the way. The photocleavable molecular pump **PcMP**$^{3+}$ consists (Figure 1a) of (i) a redox-active bipyridinium (BIPY^{2+}) unit located between (ii) a 2,6-dimethylpyridinium (PY^{+}) Coulombic barrier[17b] and (iii) an isopropylphenylene (IPP) steric barrier[17c], connected through (iv) an oligomethylene collecting chain to (v) a photocleavable stopper (PcS) by (vi) a triazole (T) ring. The choice of the photochemical cleavable stopper was based on an *o*-nitrobenzyl alcohol derivative **1** which has been used[19] widely as a photolabile protecting groups in organic[19a,19b] and polymer[19c] chemistry, and also in biology[19d]. The phenyl group on the α position (Scheme 1) introduced in **1**[20] guarantees the stopper is large enough in the pump **PcMP**$^{3+}$ to prevent the de-threading of the ring from the collecting chain. The synthesis of **PcMP**•3PF_6 was accomplished (Scheme 1) in three steps, starting from commercially available 3,4-dimethoxy-2-nitrobenzaldehyde. See Section B in Supporting Information (SI) for further details relating to the synthesis of the photocleavable molecular pump.

The redox-driven pumping process uses electricity to recruit a ring from the bulk solution by an energy ratchet mechanism[11b,21]. This mechanism relies[17,18] on the manipulation of the heights of kinetic barriers and the depths of thermodynamic wells resulting from interactions between the ring and the units of which the pumping cassette is comprised. As the ring begins the process of threading onto the pump, the Coulombic barrier presented by PY^{+} is very large if the ring is in its oxidized state but is much smaller if the ring is in its reduced state.

Furthermore, the binding interaction between the **CBPQT**$^{2(+\bullet)}$ ring and BIPY$^{+\bullet}$ is very strong[22], whereas the interaction between the **CBPQT**$^{4+}$ ring and BIPY^{2+} is repulsive (Figure 1b, I). In contrast, the barrier imposed by IPP is essentially independent of the redox state of the ring. As a result of these redox-dependent interactions, reduction followed by oxidation recruits a ring from the bulk solution and deposits it on the collecting chain, forming the [2]rotaxane **R**$^{7+}$. After the photocleavage of the stopper in **R**$^{7+}$, the ring escapes into the bulk solution completing the pumping action.

The application of a constant reduction potential of −700 mV to a reaction mixture of **PcMP**$^{3+}$ and **CBPQT**$^{4+}$ in MeCN, inside the working half-cell of a custom-built electrolysis apparatus (Section C, SI), reduces all of the BIPY^{2+} to BIPY$^{+\bullet}$ units present in both the ring and on the pump. The **CBPQT**$^{2(+\bullet)}$ ring and BIPY$^{+\bullet}$ unit enter into radical-pairing interactions, forming (Figure 1b, II) a trisradical tricationic complex[22]. Subsequent oxidation, by employing an oxidation potential of +700 mV restores the three positive charges to the pump, bringing the total charge up to +7. As a result of Coulombic repulsion, the ring passes over the IPP barrier (not over PY^{+}) onto the collecting chain in a thermally activated process, affording (Figure 1b, III) a kinetically trapped out-of-equilibrium [2]rotaxane **R**$^{7+}$. The structure of the isolated rotaxane has been confirmed by ^{1}H (Figures 2b and S2), DOSY (Figure S3) and NOESY (Figure S6) NMR spectroscopy. Comparisons of the ^{1}H NMR spectra of **PcMP**$^{3+}$ (Figure 2a) and **R**$^{7+}$ (Figure 2b) reveal a large upfield movement in the chemical shifts of the probe-resonances[23] for $H_{17'}$ through $H_{25'}$, arising from the shielding influence of the CBPQT^{4+} ring trapped on the collecting chain.

Continuous UV irradiation (365 nm) triggers the photocleavage of the stopper PcS in **R**$^{7+}$, resulting in the release (Figure 1b, IV) of the threaded ring into the bulk solution, leaving a pseudodumbbell **PDB**$^{3+}$ containing the pumping cassette[18] with a terminal carboxylic acid and the cleaved stopper **PcS***. The reaction proceeds to completion as shown (Figure 2c) by the

return of the chemical shifts[21] for H_α and H_β on **CBPQT**$^{4+}$ ring and the collecting chain (H_{17*} to H_{25*}) to their original values (Figures 2a, S2, and S5) on account of similar chemical environments experienced by **PcMP**$^{3+}$ and **PDB**$^{3+}$. This observation shows the absence of noncovalent bonding interactions between the collecting chain and the ring, thus demonstrating the complete release of the ring from the [2]rotaxane.

The release of the ring upon UV irradiation (Figure 3a) was monitored (Section D, SI) by ^{1}H NMR (Figures S7−S12) spectroscopy as follows—a solution of **R**•7PF_6 in CD_3CN (c_0 = 1 mM) was subjected to UV irradiation for 25 min, during which time a series of ^{1}H NMR spectra were recorded. The molar fractions of the resulting **R**$^{7+}$, **PDB**$^{3+}$, **PcS***, and **CBPQT**$^{4+}$ were obtained (Figure 3b) from integration of the proton resonances (Figures S10−S12) for $H_{18'}$, H_{18*}, H_{30*}, and H_α, respectively. The rate constants for both the photocleavage and ring release process—with respect to the decreased intensities of proton resonances $H_{30'}$ for the stopper PcS, and $H_{\alpha'}$ for the threaded CBPQT^{4+} ring, respectively—were found (Figure 3c) to be (0.216 ± 0.003) and (0.218 ± 0.003) min^{-1}. The identical first-order rate constants reveal that the photolysis and ring release processes occur synchronously.

The efficient and controlled release of the ring from the collecting chain was also demonstrated (Figure 4a) by fluorescence quenching experiments. The addition of 3 equiv of **R**•7PF_6 to the MeCN solution of the 1,5-dioxynaphthalene (**DNP**) fluorophore, quenched the fluorescence on account of the formation (Figure 4a) of a donor-acceptor inclusion complex[24] between **DNP** and the **CBPQT**$^{4+}$ ring released during the photolysis of the [2]rotaxane. The quenching was monitored (Figure 4b) by recording the fluorescence spectra over time. The normalized fluorescence intensities at 327 and 342 nm decreased (Figure 4b) and reached the steady state after a sum total of 18 min UV irradiation. Temporal control of the ring release process was demonstrated (Figure 4c) by switching the UV light on and off alternately.

In summary, we have demonstrated the operation of an artificial molecular pump by applying orthogonal electrical and optical stimuli sequentially. The controlled capture of the ring from the bulk solution energetically uphill using electricity and subsequent release of the ring energetically downhill using light results in the unidirectional transport of the ring onto, along, and off the dumbbell employing an energy ratchet mechanism. The fast release of the ring from the intermediate [2]rotaxane occurs synchronously with the photolysis. The current choice of the irreversible photocleavable stopper, in principles, grants access to drug delivery or cargo release platforms in which rapid and controlled-release kinetics are essential. This pump design provides increased richness for control of the relative motions of component parts in artificial molecular machines. The use of orthogonal stimuli, which introduces this higher level of control, may find applications in the integration of multiple molecular machines working in concert.

■ ASSOCIATED CONTENT

Supporting Information

Detailed information regarding the experimental methods, procedures, supportive figures and schemes. This material is available free of charge via the Internet at http://pubs.acs.org.

■ ACKNOWLEDGEMENTS

The authors thank Northwestern University for financial support. This work made use of the Integrated Molecular Structure Education and Research Center (IMSERC) at Northwestern University, which has received support from the Soft and Hybrid Nanotechnology Experimental (SHyNE) Resource (NSF ECCS-1542205), the State of Illinois, and the International Institute for Nanotechnology (IIN).

■ AUTHOR INFORMATION

Corresponding Authors

astumian@maine.edu stoddart@northwestern.edu

Notes

Guo, Q.-H.; Qiu, Y. and Stoddart, J. F. have a patent application through Northwestern University based on this work: A molecular pump powered sequentially by electricity and light.

■ REFERENCES

(1) (a) Gouaux, E.; MacKinnon, R. Principles of selective ion transport in channels and pumps. *Science* **2005**, *310*, 1461–1465. (b) Piccolino, M. Biological machines: From mills to molecules. *Nat. Rev. Mol. Cell Biol.* **2000**, *1*, 149–152. (c) Tsong, T. Y.; Astumian, R. D. Electroconformational coupling: How membrane-bound ATPase transduces energy from dynamic electric fields. *Annu. Rev. Physiol.* **1988**, *50*, 273–290.

(2) (a) Morth, J. P.; Pedersen, B. P.; Toustrup-Jensen, M. S.; Sørensen, T. L. M.; Petersen, J.; Andersen, J. P.; Vilsen, B.; Nissen, P. Crystal structure of the sodium–potassium pump. *Nature* **2007**, *450*, 1043–1049. (b) Toyoshima, C.; Nakasako, M.; Nomura, H.; Ogawa, H. Crystal structure of the calcium pump of sarcoplasmic reticulum at 2.6 Å resolution. *Nature* **2000**, *405*, 647–655. (c) Stock, D.; Leslie, A. G. W.; Walker, J. E. Molecular architecture of the rotary motor in ATP synthase. *Science* **1999**, *286*, 1700–1705.

(3) (a) Credi, A.; Balzani, V. *Molecular Machines*; 1088press: Bologna, 2020. (b) Dattler, D.; Fuks, G.; Heiser, J.; Moulin, E.; Perrot, A.; Yao, X.; Giuseppone, N. Design of collective motions from synthetic molecular switches, rotors, and motors. *Chem. Rev.* **2020**, *120*, 310–433. (c) Moulin, E.; Faour, L.; Carmona-Vargas, C. C.; Giuseppone, N. From molecular machines to stimuli-responsive materials. *Adv. Mater.* **2020**, *32*, 1906036. (d) Aprahamian, I. The future of molecular machines. *ACS Cent. Sci.* **2020**, *6*, 347–358. (e) Lancia, F.; Ryabchun, A.; Katsonis, N. Life-like motion driven by artificial molecular machines. *Nat. Rev. Chem.* **2019**, *3*, 536–551. (f) Roke, D.; Wezenberg, S. J.; Feringa, B. L. Molecular rotary motors: Unidirectional motion around double bonds. *Proc. Natl. Acad. Sci. U. S. A.* **2018**, *115*, 9423–9431. (g) Foy, J. T.; Li, Q.; Goujon, A.; Colard-Itté, J.-R.; Fuks, G.; Moulin, E.; Schiffmann, O.; Dattler, D.; Funeriu, D. P.; Giuseppone, N. Dual-light control of nanomachines that integrate motor and modulator subunits. *Nat. Nanotechnol.* **2017**, *12*, 540–545. (h) Kassem, S.; van Leeuwen, T.; Lubbe, A. S.; Wilson, M. R.; Feringa, B. L.; Leigh, D. A. Artificial Molecular Motors. *Chem. Soc. Rev.* **2017**, *46*, 2592–2621. (i) Abendroth, J. M.; Bushuyev, O. S.; Weiss, P. S.; Barrett, C. J. Controlling motion at the nanoscale: Rise of the molecular machines. *ACS Nano* **2015**, *9*, 7746–7768. (j) Credi, A.; Silvi, S.; Venturi, M. *Molecular Machines and Motors: Recent Advances and Perspectives*; Springer: Heidelberg, 2014. (k) Pathem, B. K.; Claridge,

S. A.; Zheng, Y. B.; Weiss, P. S. Molecular switches and motors on surfaces. *Annu. Rev. Phys. Chem.* **2013**, *64*, 605–630. (l) Ruangsupapichat, N.; Pollard, M. M.; Harutyunyan, S. R.; Feringa, B. L. Reversing the direction in a light-driven rotary molecular motor. *Nat. Chem.* **2011**, *3*, 53–60. (m) Balzani, V.; Credi, A.; Venturi, M. *Molecular Devices and Machines: Concepts and Perspectives for the Nanoworld*; Wiley-VCH: Weinheim, 2008. (n) Fletcher, S. P.; Dumur, F.; Pollard, M. M.; Feringa, B. L. A reversible, unidirectional molecular rotary motor driven by chemical energy. *Science* **2005**, *310*, 80–82. (o) Berná, J.; Leigh, D. A.; Lubomska, M.; Mendoza, S. M.; Pérez, E. M.; Rudolf, P.; Teobaldi, G.; Zerbetto, F. Macroscopic transport by synthetic molecular machines. *Nat. Mater.* **2005**, *4*, 704–710. (p) Balzani, V.; Credi, A.; Raymo, F. M.; Stoddart, J. F. Artificial molecular machines. *Angew. Chem., Int. Ed.* **2000**, *39*, 3348–3391.

(4) (a) Feringa, B. L. The art of building small: From molecular switches to motors (Nobel Lecture). *Angew. Chem., Int. Ed.* **2017**, *56*, 11060–11078. (b) Sauvage, J.-P. From chemical topology to molecular machines (Nobel Lecture). *Angew. Chem., Int. Ed.* **2017**, *56*, 11080–11093. (c) Cheng, C.; Stoddart, J. F. Wholly synthetic molecular machines. *ChemPhysChem* **2016**, *17*, 1780–1793. (d) Leigh, D. A. Genesis of the nanomachines: The 2016 Nobel Prize in chemistry. *Angew. Chem., Int. Ed.* **2016**, *55*, 14506–14508. (e) Erbas-Cakmak, S.; Leigh, D. A.; McTernan, C. T.; Nussbaumer, A. L. Artificial molecular machines. *Chem. Rev.* **2015**, *115*, 10081–10206. (f) Szymański, W.; Beierle, J. M.; Kistemaker, H. A. V.; Velema, W. A.; Feringa, B. L. Reversible photocontrol of biological systems by the incorporation of molecular photoswitches. *Chem. Rev.* **2013**, *113*, 6114–6178. (g) Leigh, D. A.; Wong, J. K. Y.; Dehez, F.; Zerbetto, F. Unidirectional rotation in a mechanically interlocked molecular rotor. *Nature* **2003**, *424*, 174–179. (h) Koumura, N.; Zijlstra, R. W. J.; van Delden, R. A.; Harada, N.; Feringa, B. L. Light-driven monodirectional molecular rotor. *Nature* **1999**, *401*, 152–155.

(5) Stoddart, J. F. Unnatural product synthesis. *Nature* **1988**, *334*, 10–11.

(6) (a) Sluysmans, D.; Stoddart, J. F. The burgeoning of mechanically interlocked molecules in chemistry. *Trends Chem.* **2019**, *1*, 185-197. (b) Stoddart, J. F. Mechanically interlocked molecules (MIMs)—Molecular shuttles, switches, and machines (Nobel Lecture). *Angew. Chem., Int. Ed.* **2017**, *56*, 11094–11125.

(7) (a) Heard, A. W.; Goldup, S. M. Synthesis of a mechanically planar chiral rotaxane ligand for enantioselective catalysis. *Chem* **2020**, *6*, 994–1006. (b) Van Raden, J. M.; White, B. M.; Zakharov, L. N.; Jasti, R. Nanohoop rotaxanes from active metal template syntheses and their potential in sensing applications. *Angew. Chem., Int. Ed.* **2019**, *58*, 7341–7345. (c) Jinks, M. A.; de Juan, A.; Denis, M.; Fletcher, C. J.; Galli, M.; Jamieson, E. M. G.; Modicom, F.; Zhang,

Z.; Goldup, S. M. Stereoselective synthesis of mechanically planar chiral rotaxanes. *Angew. Chem., Int. Ed.* **2018**, *57*, 14806–14810. (d) Denis, M.; Pancholi, J.; Jobe, K.; Watkinson, M.; Goldup, S. M. Chelating rotaxane ligands as fluorescent sensors for metal ions. *Angew. Chem., Int. Ed.* **2018**, *57*, 5310–5314. (e) De Bo, G.; Gall, M. A. Y.; Kuschel, S.; De Winter, J.; Gerbaux, P.; Leigh, D. A. An artificial molecular machine that builds an asymmetric catalyst. *Nat. Nanotechnol.* **2018**, *13*, 381–385. (f) Goujon, A.; Lang, T.; Mariani, G.; Moulin, E.; Fuks, G.; Raya, J.; Buhler, E.; Giuseppone, N. Bistable [*c*2] daisy chain rotaxanes as reversible muscle-like actuators in mechanically active gels. *J. Am. Chem. Soc.* **2017**, *139*, 14825–14828. (g) Lewandowski, B.; De Bo, G.; Ward, J. W.; Papmeyer, M.; Kuschel, S.; Aldegunde, M. J.; Gramlich, P. M. E.; Heckmann, D.; Goldup, S. M.; D'Souza, D. M.; Fernandes, A. E.; Leigh, D. A. Sequence-specific peptide synthesis by an artificial small-molecule machine. *Science* **2013**, *339*, 189–193. (h) Balzani, V.; Clemente-León, M.; Credi, A.; Ferrer, B.; Venturi, M.; Flood, A. H.; Stoddart, J. F. Autonomous artificial nanomotor powered by sunlight. *Proc. Natl. Acad. Sci. U. S. A.* **2006**, *103*, 1178–1183. (i) Badjić, J. D.; Balzani, V.; Credi, A.; Silvi, S.; Stoddart, J. F. A molecular elevator. *Science* **2004**, *303*, 1845–1849. (j) Bissell, R. A.; Córdova, E.; Kaifer, A. E.; Stoddart, J. F. A chemically and electrochemically switchable molecular shuttle. *Nature* **1994**, *369*, 133–137.

(8) (a) Denis, M.; Lewis, J. E. M.; Modicom, F.; Goldup, S. M. An auxiliary approach for the stereoselective synthesis of topologically chiral catenanes. *Chem* **2019**, *5*, 1512–1520. (b) Segawa, Y.; Kuwayama, M.; Hijikata, Y.; Fushimi, M.; Nishihara, T.; Pirillo, J.; Shirasaki, J.; Kubota, N.; Itami, K. Topological molecular nanocarbons: All-benzene catenane and trefoil knot. *Science* **2019**, *365*, 272–276. (c) Nguyen, M. T.; Ferris, D. P.; Pezzato, C.; Wang, Y.; Stoddart, J. F. Densely charged dodecacationic [3]- and tetracosacationic radial [5]catenanes. *Chem* **2018**, *4*, 2329-2344. (d) Erbas-Cakmak, S.; Fielden, S. D. P.; Karaca, U.; Leigh, D. A.; McTernan, C. T.; Tetlow, D. J.; Wilson, M. R. Rotary and linear molecular motors driven by pulses of a chemical fuel. *Science* **2017**, *358*, 340–343. (e) Wilson, M. R.; Solà, J.; Carlone, A.; Goldup, S. M.; Lebrasseur, N.; Leigh, D. A. An autonomous chemically fuelled small-molecule motor. *Nature* **2016**, *534*, 235–240. (f) Hernández, J. V.; Kay, E. R.; Leigh, D. A. A reversible synthetic rotary molecular motor. *Science* **2004**, *306*, 1532–1537. (g) Balzani, V.; Credi, A.; Langford, S. J.; Raymo, F. M.; Stoddart, J. F.; Venturi, M. Constructing molecular machinery: A chemically-switchable [2]catenane. *J. Am. Chem. Soc.* **2000**, *122*, 3542–3543. (h) Asakawa, M.; Ashton, P. R.; Balzani, V.; Credi, A.; Hamers, C.; Mattersteig, G.; Montalti, M.; Shipway, A. N.; Spencer, N.; Stoddart, J. F.; Tolley, M. S.; Venturi, M.; White, A. J. P.; Williams, D. J.

A chemically and electrochemically switchable [2]catenane incorporating a tetrathiafulvalene unit. *Angew. Chem., Int. Ed.* **1998**, *37*, 333–337.

(9) (a) Heard, A. W.; Goldup, S. M. Simplicity in the design, operation, and applications of mechanically interlocked molecular machines. *ACS Cent. Sci.* **2020**, *6*, 117–128. (b) Zhang, L.; Marcos, V.; Leigh, D. A. Molecular machines with bio-inspired mechanisms. *Proc. Natl. Acad. Sci. U. S. A.* **2018**, *115*, 9397–9404.

(10) Bruns, C. J.; Stoddart, J. F. *The Nature of the Mechanical Bond: From Molecules to Machines*; Wiley: Hoboken, New Jersey, 2016.

(11) (a) Astumian, R. D.; Pezzato, C.; Feng, Y.; Qiu, Y.; McGonigal, P. R.; Cheng, C.; Stoddart, J. F. Non-equilibrium kinetics and trajectory thermodynamics of synthetic molecular pumps. *Mater. Chem. Front.* **2020**, *4*, 1304–1314. (b) Pezzato, C.; Cheng, C.; Stoddart, J. F.; Astumian, R. D. Mastering the non-equilibrium assembly and operation of molecular machines. *Chem. Soc. Rev.* **2017**, *46*, 5491–5507. (c) Astumian, R. D. Design principles for Brownian molecular machines: How to swim in molasses and walk in a hurricane. *Phys. Chem. Chem. Phys.* **2007**, *9*, 5067–5083.

(12) (a) Müller-Dethlefs, K.; Hobza, P. Noncovalent interactions: A challenge for experiment and theory. *Chem. Rev.* **2000**, *100*, 143–168. (b) Lehn, J.-M. Supramolecular chemistry—Scope and perspectives molecules, supermolecules, and molecular devices (Nobel Lecture). *Angew. Chem., Int. Ed. Engl.* **1988**, *27*, 89–112. (c) Cram, D. J. The design of molecular hosts, guests, and their complexes (Nobel Lecture). *Angew. Chem. Int. Ed. Engl.* **1988**, *27*, 1009–1020.

(13) (a) Zhou, H.-Y.; Han, Y.; Chen, C.-F. pH-Controlled motions in mechanically interlocked molecules. *Mater. Chem. Front.* **2020**, *4*, 12–28. (b) Zhou, H.-Y.; Han, Y.; Shi, Q.; Chen, C.-F. Directional transportation of a helic[6]arene along a nonsymmetric molecular axle. *J. Org. Chem.* **2019**, *84*, 5872–5876. (c) Biagini, C.; Fielden, S. D. P.; Leigh, D. A.; Schaufelberger, F.; Di Stefano, S.; Thomas, D. Dissipative catalysis with a molecular machine. *Angew. Chem., Int. Ed.* **2019**, *58*, 9876–9880. (d) Meng, Z.; Xiang, J.-F.; Chen, C.-F. Directional molecular transportation based on a catalytic stopper-leaving rotaxane system. *J. Am. Chem. Soc.* **2016**, *138*, 5652–5658. (e) Carlone, A.; Goldup, S. M.; Lebrasseur, N.; Leigh, D. A.; Wilson, A. A three-compartment chemically-driven molecular information ratchet. *J. Am. Chem. Soc.* **2012**, *134*, 8321–8323. (f) Alvarez-Pérez, M.; Goldup, S. M.; Leigh, D. A.; Slawin, A. M. Z. A chemically-driven molecular information ratchet. *J. Am. Chem. Soc.* **2008**, *130*, 1836–1838.

(14) (a) Schröder, Hendrik V.; Schalley, C. A. Electrochemically switchable rotaxanes: recent strides in new directions. *Chem. Sci.* **2019**, *10*, 9626-9639. (b) Pezzato, C.; Nguyen, M. T.;

Kim, D. J.; Anamimoghadam, O.; Mosca, L.; Stoddart, J. F. Controlling dual molecular pumps electrochemically. *Angew. Chem., Int. Ed.* **2018**, *57*, 9325–9329. (c) Ragazzon, G.; Schäfer, C.; Franchi, P.; Silvi, S.; Colasson, B.; Lucarini, M.; Credi, A. Remote electrochemical modulation of pK_a in a rotaxane by co-conformational allostery. *Proc. Natl. Acad. Sci. U. S. A.* **2018**, *115*, 9385–9390. (d) Ragazzon, G.; Baroncini, M.; Ceroni, P.; Credi, A.; Venturi, M. *Electrochemically Controlled Supramolecular Switches and Machines*; Elsevier: Oxford, 2017. (e) McGonigal, P. R.; Deria, P.; Hod, I.; Moghadam, P. Z.; Avestro, A.-J.; Horwitz, N. E.; Gibbs-Hall, I. C.; Blackburn, A. K.; Chen, D.; Botros, Y. Y.; Wasielewski, M. R.; Snurr, R. Q.; Hupp, J. T.; Farha, O. K.; Stoddart, J. F. Electrochemically addressable trisradical rotaxanes organized within a metal–organic framework. *Proc. Natl. Acad. Sci. U. S. A.* **2015**, *112*, 11161–11168. (f) Bruns, C. J.; Li, J.; Frasconi, M.; Schneebeli, S. T.; Iehl, J.; Jacquot de Rouville, H.-P.; Stupp, S. I.; Voth, G. A.; Stoddart, J. F. An electrochemically and thermally switchable donor–acceptor [*c*2]daisy chain rotaxane. *Angew. Chem., Int. Ed.* **2014**, *53*, 1953–1958. (g) Venturi, M.; Credi, A. Electroactive [2]catenanes. *Electrochim. Acta* **2014,** *140*, 467–475. (h) Ye, T.; Kumar, A. S.; Saha, S.; Takami, T.; Huang, T. J.; Stoddart, J. F.; Weiss, P. S. Changing stations in single bistable rotaxane molecules under electrochemical control. *ACS Nano* **2010**, *4*, 3697–3701. (i) Juluri, B. K.; Kumar, A. S.; Liu, Y.; Ye, T.; Yang, Y.-W.; Flood, A. H.; Fang, L.; Stoddart, J. F.; Weiss, P. S.; Huang, T. J. A mechanical actuator driven electrochemically by artificial molecular muscles. *ACS Nano* **2009**, *3*, 291–300. (j) Fioravanti, G.; Haraszkiewicz, N.; Kay, E. R.; Mendoza, S. M.; Bruno, C.; Marcaccio, M.; Wiering, P. G.; Paolucci, F.; Rudolf, P.; Brouwer, A. M.; Leigh, D. A. Three state redox-active molecular shuttle that switches in solution and on a surface. *J. Am. Chem. Soc.* **2008**, *130*, 2593–2601. (k) Saha, S.; Flood, A. H.; Stoddart, J. F.; Impellizzeri, S.; Silvi, S.; Venturi, M.; Credi, A. A redox-driven multicomponent molecular shuttle. *J. Am. Chem. Soc.* **2007**, *129*, 12159–12171. (l) Deng, W.-Q.; Flood, A. H.; Stoddart, J. F.; Goddard, III, W. A. An electrochemical color-switchable RGB dye: Tristable [2]catenane. *J. Am. Chem. Soc.* **2005**, *127*, 15994–15995. (m) Altieri, A.; Gatti, F. G.; Kay, E. R.; Leigh, D. A.; Martel, D.; Paolucci, F.; Slawin, A. M. Z.; Wong, J. K. Y. Electrochemically switchable hydrogen-bonded molecular shuttles. *J. Am. Chem. Soc.* **2003**, *125*, 8644–8654. (n) Livoreil, A.; Dietrich-Buchecker, C. O.; Sauvage, J.-P. Electrochemically triggered swinging of a [2]-catenate. *J. Am. Chem. Soc.* **1994**, *116*, 9399–9400.

(15) (a) Corra, S.; Curcio, M.; Baroncini, M.; Silvi, S.; Credi, A. Photoactivated artificial molecular machines that can perform tasks. *Adv. Mater.* **2020**, *32*, 1906064. (b) García-López, V.; Liu, D.; Tour, J. M. Light-activated organic molecular motors and their applications. *Chem. Rev.* **2020**, *120*, 79–124. (c) Chen, S.; Leung, F. K.-C.; Stuart, M. C. A.; Wang, C.; Feringa, B.

L. Dynamic assemblies of molecular motor amphiphiles control macroscopic foam properties. *J. Am. Chem. Soc.* **2020**, *142*, 10163–10172. (d) Sabatino, A.; Penocchio, E.; Ragazzon, G.; Credi, A.; Frezzato, D. Individual-molecule perspective analysis of chemical reaction networks: The case of a light-driven supramolecular pump. *Angew. Chem., Int. Ed.* **2019**, *58*, 14341–14348. (e) Groppi, J.; Baroncini, M.; Venturi, M.; Silvi, S.; Credi, A. Design of photo-activated molecular machines: Highlights from the past ten years. *Chem. Commun.* **2019**, *55*, 12595–12602. (f) Moran, M. J.; Magrini, M.; Walba, D. M.; Aprahamian, I. Driving a liquid crystal phase transition using a photochromic hydrazone. *J. Am. Chem. Soc.* **2018**, *140*, 13623–13627. (g) Shao, B.; Baroncini, M.; Qian, H.; Bussotti, L.; Di Donato, M.; Credi, A.; Aprahamian, I. Solution and solid-state emission toggling of a photochromic hydrazone. *J. Am. Chem. Soc.* **2018**, *140*, 12323–12327. (h) Shi, Q.; Meng, Z.; Xiang, J.-F.; Chen, C.-F. Efficient control of movement in non-photoresponsive molecular machines by a photo-induced proton-transfer strategy. *Chem. Commun.* **2018**, *54*, 3536–3539. (i) Chen, J.; Leung, F. K.-C.; Stuart, M. C. A.; Kajitani, T.; Fukushima, T.; van der Giessen, E.; Feringa, B. L. Artificial muscle-like function from hierarchical supramolecular assembly of photoresponsive molecular motors. *Nat. Chem.* **2018**, *10*, 132–138. (j) Gao, C.; Luan, Z.-L.; Zhang, Q.; Yang, S.; Rao, S.-J.; Qu, D.-H.; Tian, H. Triggering a [2]rotaxane molecular shuttle by a photochemical bond-cleavage strategy. *Org. Lett.* **2017**, *19*, 1618–1621. (k) Qian, H.; Pramanik, S.; Aprahamian, I. Photochromic hydrazone switches with extremely long thermal half-lives. *J. Am. Chem. Soc.* **2017**, *139*, 9140–9143. (l) Ragazzon, G.; Baroncini, M.; Silvi, S.; Venturi, M.; Credi, A. Light-powered autonomous and directional molecular motion of a dissipative self-assembling system. *Nat. Nanotechnol.* **2015**, *10*, 70–75. (m) Tatum, L. A.; Foy, J. T.; Aprahamian, I. Waste management of chemically activated switches: Using a photoacid to eliminate accumulation of side products. *J. Am. Chem. Soc.* **2014**, *136*, 17438–17441. (n) Serreli, V.; Lee, C.-F.; Kay, E. R.; Leigh, D. A. A molecular information ratchet. *Nature* **2007**, *445*, 523–527. (o) Ballardini, R.; Balzani, V.; Clemente-León, M.; Credi, A.; Gandolfi, M. T.; Ishow, E.; Perkins, J.; Stoddart, J. F.; Tseng, H.-R.; Wenger, S. Photoinduced electron transfer in a triad that can be assembled/disassembled by two different external inputs. Toward molecular-level electrical extension cables. *J. Am. Chem. Soc.* **2002**, *124*, 12786–12795. (p) Brouwer, A. M.; Frochot, C.; Gatti, F. G.; Leigh, D. A.; Mottier, L.; Paolucci, F.; Roffia, S.; Wurpel, G. W. H. Photoinduction of fast, reversible translational motion in a hydrogen-bonded molecular shuttle. *Science* **2001**, *291*, 2124–2128. (q) Ashton, P. R.; Ballardini, R.; Balzani, V.; Credi, A.; Dress, K. R.; Ishow, E.; Kleverlaan, C. J.; Kocian, O.; Preece, J. A.; Spencer, N.; Stoddart, J. F.; Venturi, M.; Wenger, S. A photochemically driven molecular-level abacus. *Chem. Eur. J.* **2000**,

6, 3558–3574. (r) Asakawa, M.; Ashton, P. R.; Balzani, V.; Brown, C. L.; Credi, A.; Matthews, O. A.; Newton, S. P.; Raymo, F. M.; Shipway, A. N.; Spencer, N.; Quick, A.; Stoddart, J. F.; White, A. J. P.; Williams, D. J. Photoactive azobenzene-containing supramolecular complexes and related interlocked molecular compounds. *Chem. Eur. J.* **1999**, *5*, 860–875. (s) Livoreil, A.; Sauvage, J.-P.; Armaroli, N.; Balzani, V.; Flamigni, L.; Ventura, B. Electrochemically and photochemically driven ring motions in a disymmetrical copper [2]-catenate. *J. Am. Chem. Soc.* **1997**, *119*, 12114–12124. (t) Ballardini, R.; Balzani, V.; Gandolfi, M. T.; Prodi, L.; Venturi, M.; Philp, D.; Ricketts, H. G.; Stoddart, J. F. A photochemically driven molecular machine. *Angew. Chem., Int. Ed. Engl.* **1993**, *32*, 1301–1303.

(16) Baroncini, M.; Silvi, S.; Credi, A. Photo- and redox-driven artificial molecular motors. *Chem. Rev.* **2020**, *120*, 200–268.

(17) (a) Qiu, Y.; Zhang, L.; Pezzato, C.; Feng, Y.; Li, W.; Nguyen, M. T.; Cheng, C.; Shen, D.; Guo, Q.-H.; Shi, Y.; Cai, K.; Alsubaie, F. M.; Astumian, R. D.; Stoddart, J. F. A molecular dual pump. *J. Am. Chem. Soc.* **2019**, *141*, 17472–17476. (b) Pezzato, C.; Nguyen, M. T.; Cheng, C.; Kim, D. J.; Otley, M. T.; Stoddart, J. F. An efficient artificial molecular pump. *Tetrahedron* **2017**, *73*, 4849–4857. (c) Cheng, C.; McGonigal, P. R.; Schneebeli, S. T.; Li, H.; Vermeulen, N. A.; Ke, C.; Stoddart, J. F. An artificial molecular pump. *Nat. Nanotechnol.* **2015**, *10*, 547–553. (d) Li, H.; Cheng, C.; McGonigal, P. R.; Fahrenbach, A. C.; Frasconi, M.; Liu, W.-G.; Zhu, Z.; Zhao, Y.; Ke, C.; Lei, J.; Young, R. M.; Dyar, S. M.; Co, D. T.; Yang, Y.-W.; Botros, Y. Y.; Goddard, III, W. A.; Wasielewski, M. R.; Astumian, R. D.; Stoddart, J. F. Relative unidirectional translation in an artificial molecular assembly fueled by light. *J. Am. Chem. Soc.* **2013**, *135*, 18609–18620.

(18) (a) Qiu, Y.; Song, B.; Pezzato, C.; Shen, D.; Liu, W.; Zhang, L.; Feng, Y.; Guo, Q.-H.; Cai, K.; Li, W.; Chen, H.; Nguyen, M. T.; Shi, Y.; Cheng, C.; Astumian, R. D.; Li, X.; Stoddart, J. F. A precise polyrotaxane synthesizer. *Science* **2020**, *368*, 1247–1253. (b) Astumian, R. D. Kinetic asymmetry allows macromolecular catalysts to drive an information ratchet. *Nat. Commun.* **2019**, *10*, 3837. (c) Astumian, R. D.; Robertson, B. Imposed oscillations of kinetic barriers can cause an enzyme to drive a chemical reaction away from equilibrium. *J. Am. Chem. Soc.* **1993**, *115*, 11063–11068.

(19) (a) Hansen, M. J.; Velema, W. A.; Lerch, M. M.; Szymanski, W.; Feringa, B. L. Wavelength-selective cleavage of photoprotecting groups: Strategies and applications in dynamic systems. *Chem. Soc. Rev.* **2015**, *44*, 3358–3377. (b) Patchornik, A.; Amit, B.; Woodward, R. B. Photosensitive protecting groups. *J. Am. Chem. Soc.* **1970**, *92*, 6333–6335. (c) Zhao, H.; Sterner, E. S.; Coughlin, E. B.; Theato, P. o-Nitrobenzyl alcohol derivatives:

opportunities in polymer and materials science. *Macromolecules* **2012**, *45*, 1723–1736. (d) Klán, P.; Šolomek, T.; Bochet, C. G.; Blanc, A.; Givens, R.; Rubina, M.; Popik, V.; Kostikov, A.; Wirz, J. Photoremovable protecting groups in chemistry and biology: Reaction mechanisms and efficacy. *Chem. Rev.* **2013**, *113*, 119–191.

(20) Serafinowski, P. J.; Garland, P. B. Novel photoacid generators for photodirected oligonucleotide synthesis. *J. Am. Chem. Soc.* **2003,** *125*, 962−965.

(21) Astumian, R. D.; Derényi, I. Fluctuation driven transport and models of molecular motors and pumps. *Eur. Biophys. J.* **1998**, *27*, 474–489.

(22) Trabolsi, A.; Khashab, N.; Fahrenbach, A. C.; Friedman, D. C.; Colvin, M. T.; Coti, K. K.; Benitez, D.; Tkatchouk, E.; Olsen, J. C.; Belowich, M. E.; Carmielli, R.; Khatib, H. A.; Goddard, III, W. A.,; Wasielewski, M. R.; Stoddart, J. F. Radically enhanced molecular recognition. *Nat. Chem.* **2010,** *2*, 42–49.

(23) Proton resonances for $\mathbf{R}^{7+}$ and its corresponding photocleaved compounds ($\mathbf{PDB}^{3+}$ and **PcS***) are labeled with prime and star symbols, respectively.

(24) Asakawa, M.; Dehaen, W.; Labbe, G.; Menzer, S.; Nouwen, J.; Raymo, F. M.; Stoddart, J. F.; Williams, D. J. Improved template-directed synthesis of cyclobis(paraquat-*p*-phenylene). *J. Org. Chem.* **1996**, *61*, 9591–9595.

Captions to Scheme and Figures

Scheme 1. Synthesis of the photocleavable molecular pump **PcMP•**$3PF_6$

Figure 1. The design and operation of $\mathbf{PcMP}^{3+}$ powered sequentially by electricity and light. (**a**) Graphical representations and structural formulas of $\mathbf{CBPQT}^{4+}$, $\mathbf{PcMP}^{3+,}$ and the photo-cleaved units, $\mathbf{PDB}^{3+}$ and **PcS***. The key protons on the $\mathbf{PcMP}^{3+}$ (1−34), $\mathbf{CBPQT}^{4+}$ (CH_2, α, β, and Xyl), $\mathbf{PDB}^{3+}$ (17*−25*), and **PcS*** (28*−34*) are labeled in order to aid the interpretation of the ^{1}H NMR spectra (Figure 2) recorded in CD_3CN. (**b**) Graphical representations of the unidirectional transport of a ring onto, along, and off the dumbbell and the associated energy profiles in which the green and red curved arrows indicate kinetically favored and disfavored transitions, respectively. In Stage I, the positively charged ring cannot thread onto the dumbbell because of strong Coulombic repulsions with PY^+ and steric interactions with the PcS. In Stage II, reduction by a negative potential of −700 mV lowers the Coulombic barrier and favors the formation of a stable trisradical tricationic complex. In Stage III, oxidation by a positive potential of +700 mV destabilizes the interaction between the ring and the recognition site while simultaneously restoring the Coulombic barrier arising from PY^+, preventing the escape of the ring into the bulk solution. The ring must thus pass over the steric barrier IPP and thread on the collecting chain. In Stage IV, photocleavage of the stopper PcS upon UV irradiation allows the ring to return to the bulk solution.

Figure 2. ^{1}H NMR Spectra (500 MHz, CD_3CN, 298 K) of (**a**) **PcMP•**$3PF_6$, (**b**) the isolated [2]rotaxane **R•**$7PF_6$, and (**c**) a physical mixture of **PDB•**$3PF_6$, **CBPQT•**$4PF_6$, and **PcS***

resulting from UV irradiation of $\mathbf{R}^{7+}$ for 25 min. For full assignments, see Figures S1 and S4 in the Supporting Information.

Figure 3. Kinetic analysis of ring release as monitored by ^{1}H NMR spectroscopy. (**a**) Graphical illustration of the ring release following UV irradiation. (**b**) Plots of molar fractions of $\mathbf{R}^{7+}$, $\mathbf{PDB}^{3+}$, **PcS***, and $\mathbf{CBPQT}^{4+}$ with time during photocleavage. (**c**) Plots of the ln(*c*) versus time where *c* is the concentration of either $CBPQT^{4+}$ (green squares) or PcS (blue circles).

Figure 4. Kinetic analysis of ring release as monitored by fluorescence quenching. (**a**) Graphical illustration of ring release in the presence of a **DNP** fluorophore. (**b**) A stack of fluorescence spectra taken at different times. Inset: The normalized fluorescence intensities at 327 and 342 nm as a function of the irradiation time. (**c**) Illustration of temporal control where the light is turned on and off as indicated by the gray bars.

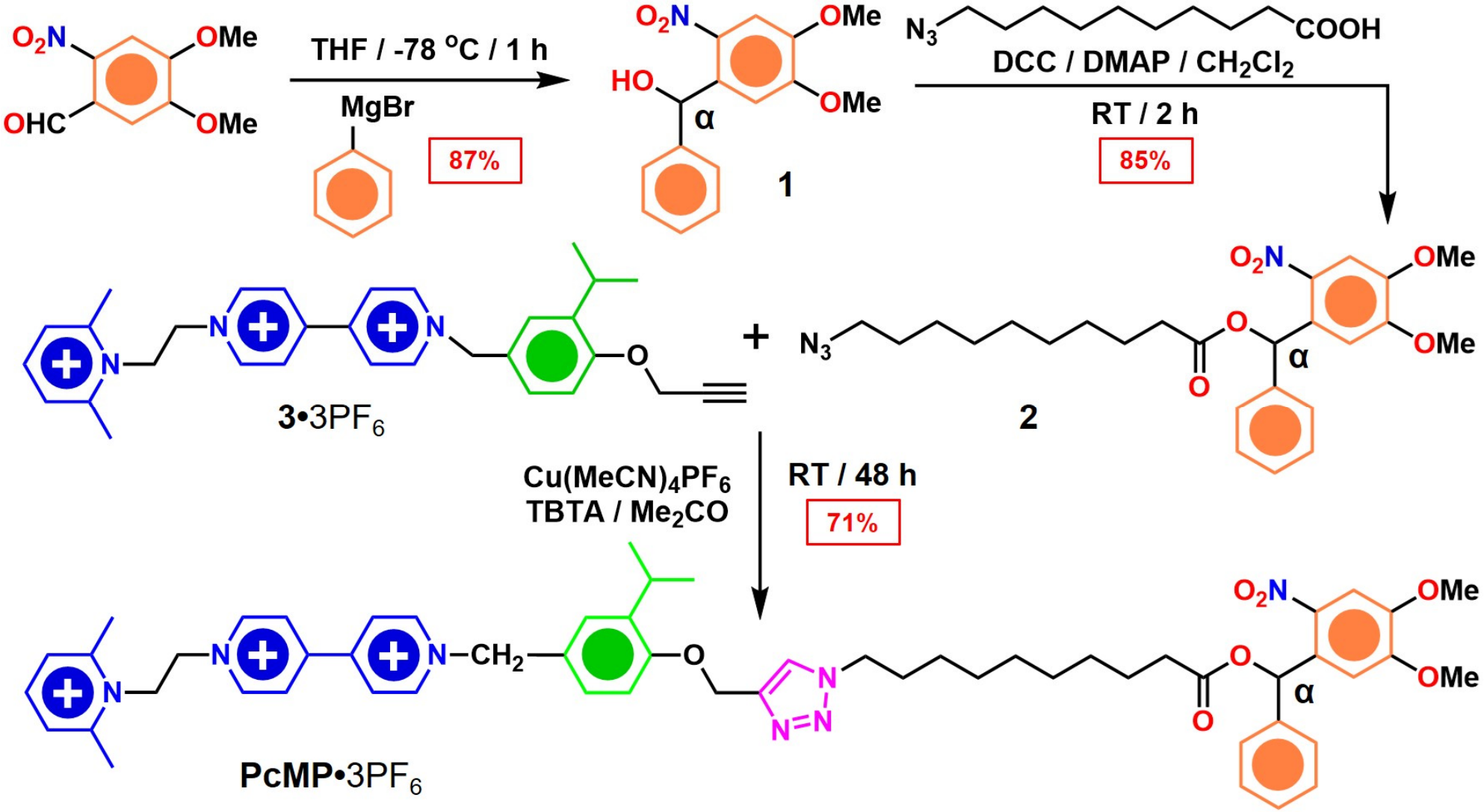
THF / -78 °C / 1 h
MgBr
87%
1
DCC / DMAP / CH2Cl2
RT / 2 h
85%
3•3PF6
2
Cu(MeCN)4PF6
TBTA / Me2CO
RT / 48 h
71%
PcMP•3PF6

Scheme 1

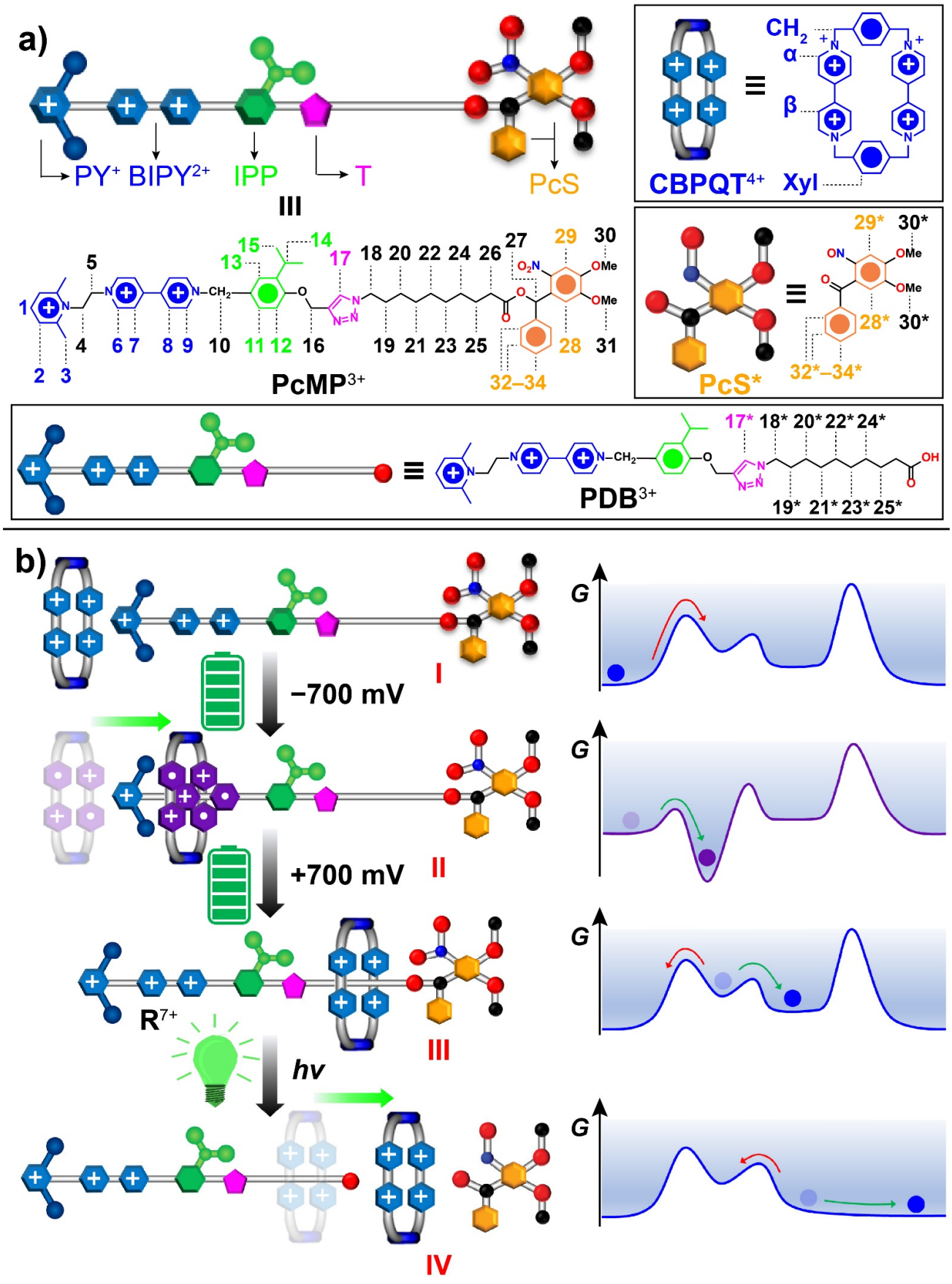
a)
PY+ BIPY2+ IPP T
PcS
III
CBPQT4+
CH2
α
β
Xyl
PcMP3+
PcS*
PDB3+
b)
I
−700 mV
II
+700 mV
R7+
III
hv
IV
G

Figure 1

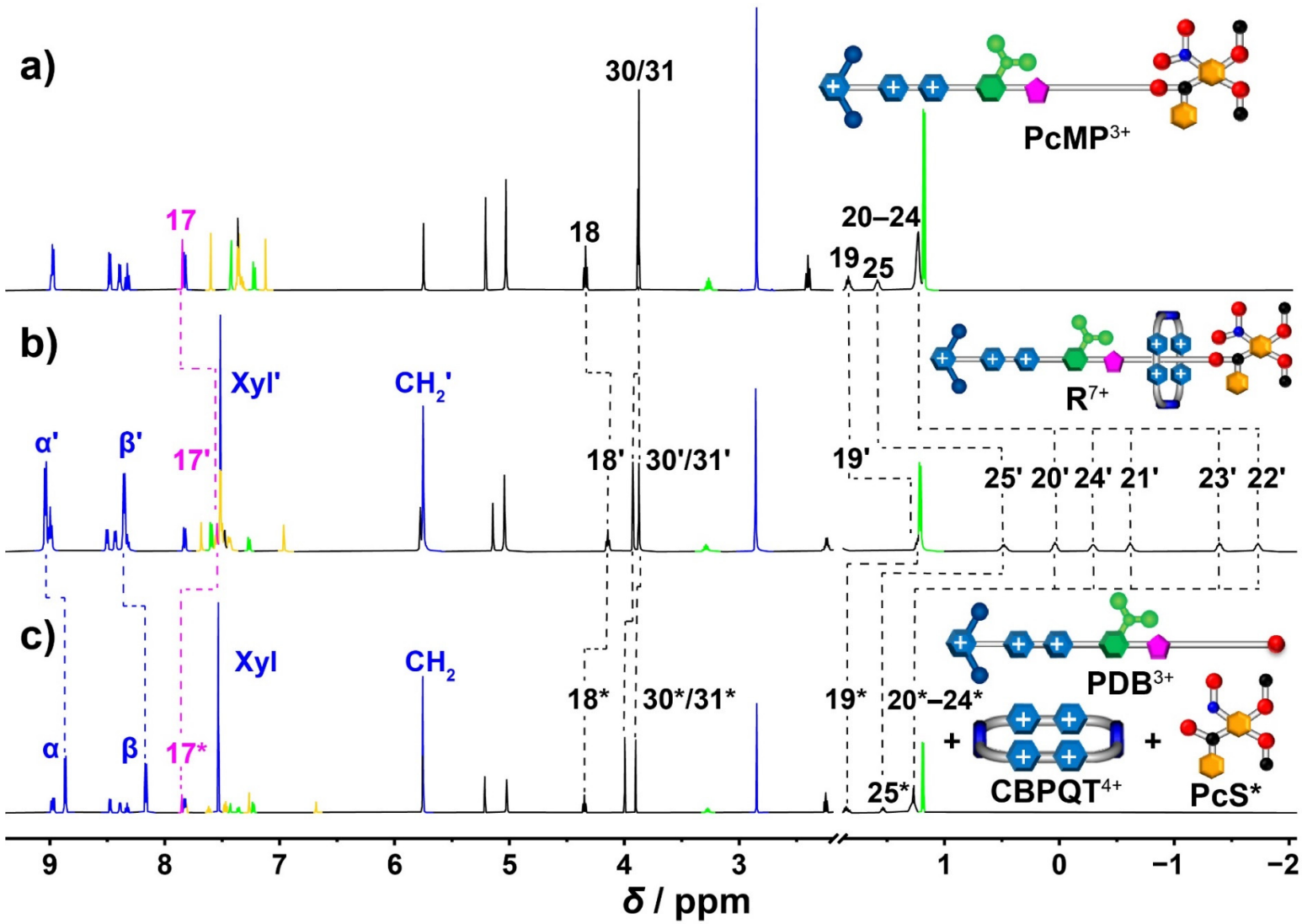
a)
30/31
PcMP3+
17
18
20–24
19
25
b)
Xyl'
CH2'
α'
β'
17'
18'
30'/31'
19'
25' 20' 24' 21'
23' 22'
R7+
c)
Xyl
CH2
α
β
17*
18*
30*/31*
19*
20*–24*
25*
PDB3+
CBPQT4+
PcS*
9 8 7 6 5 4 3 1 0 −1 −2
δ / ppm

Figure 2

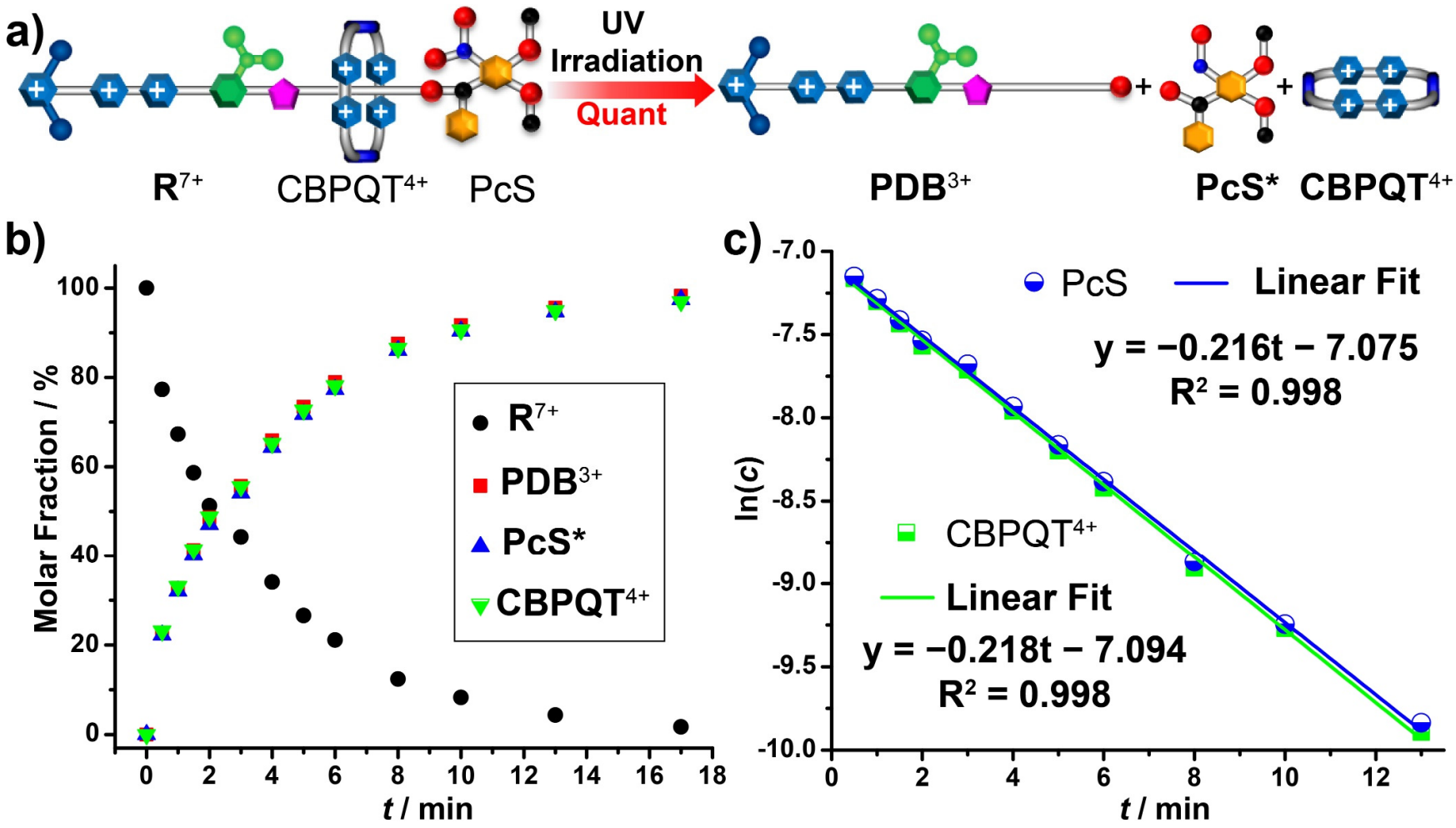
a)
UV
Irradiation
Quant
R7+
CBPQT4+
PcS
PDB3+
PcS*
CBPQT4+
b)
Molar Fraction / %
t / min
R7+
PDB3+
PcS*
CBPQT4+
c)
ln(c)
t / min
PcS
Linear Fit
y = −0.216t − 7.075
R² = 0.998
CBPQT4+
Linear Fit
y = −0.218t − 7.094
R² = 0.998

Figure 3

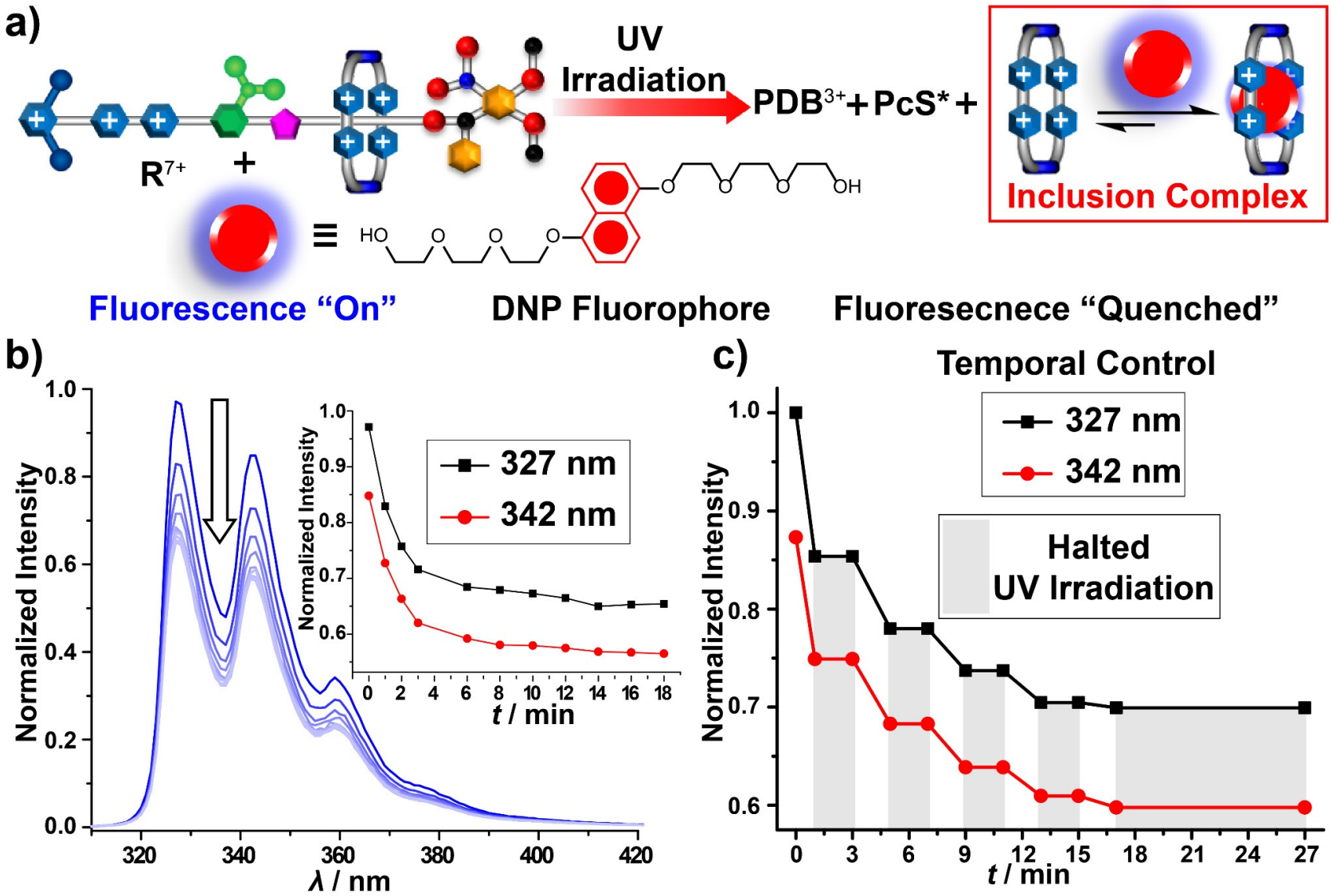
a)
UV
Irradiation
PDB3+ + PcS* +
R7+
+
≡
HO
OH
Inclusion Complex
Fluorescence "On"
DNP Fluorophore
Fluoresecnece "Quenched"
b)
Normalized Intensity
λ / nm
327 nm
342 nm
t / min
c)
Temporal Control
Halted
UV Irradiation
t / min

Figure 4

Table of Contents Graphic